

Faculty of Informatics

Faculty of Informatics - Papers

University of Wollongong

Year 2006

Improved Three-step Phase Shifting Profilometry Using Digital Fringe Pattern Projection

Y. Hu*

J. Xi†

J. F. Chicharo‡

Z. Yang**

*University of Wollongong, yingsong@uow.edu.au

†University of Wollongong, jiangtao@uow.edu.au

‡University of Wollongong, chicharo@uow.edu.au

**Huazhong University of Science & Technology, China

This article was originally published as: Hu, Y, Xi, J, Chicharo, J & Yang, Z, Improved Three-step Phase Shifting Profilometry Using Digital Fringe Pattern Projection, International Conference on Computer Graphics, Imaging and Visualisation 2006, 26-28 July 2006, 161-167. Copyright IEEE 2006.

This paper is posted at Research Online.

<http://ro.uow.edu.au/infopapers/461>

Improved Three-step Phase Shifting Profilometry Using Digital Fringe Pattern Projection

Yingsong Hu^{1,2}, Jiangtao Xi^{1,2}, Joe Chicharo¹ and Zongkai Yang²

¹School of Electrical Computer and Telecommunications Engineering,
University of Wollongong, NSW 2522, Australia.

²Department of Electronic and Information Engineering,
Huazhong University of Science and Technology, Wuhan City, 430074, China.

Abstract

In this paper, an improved method for three-step phase shifting profilometry (PSP) is presented to eliminate the errors introduced by the second order harmonic when digital projection are used to generate fringe patterns. Firstly, the error caused by the second order harmonic is theoretically analyzed. Then based on the error analysis and principle of PSP, we propose a novel approach, called improved three-step phase shifting profilometry (I3PSP), to eliminate the influence of the second order harmonic. Finally, simulations are performed to verify the effectiveness of the proposed I3PSP, which demonstrate that the reconstruction accuracy of using three-step PSP has been significantly improved by the proposed I3PSP.

1 Introduction

Fringe pattern profilometry (FPP) is one of the most popular non-contact approaches to reconstructing three-dimensional object surfaces. With FPP, a Ronchi grating or sinusoidal grating is projected onto a three-dimensional diffuse surface, the height distribution of which deforms the projected fringe patterns and modulates them in phase domain. Hence by retrieving the phase difference between the original and deformed fringe patterns, three-dimensional profilometry can be achieved. In order to obtain phase maps from original and deformed fringes patterns, researchers contributed various analysis methods, including Fourier transform profilometry(FTP) [2, 13, 14, 16, 17, 20], phase shifting profilometry (PSP) [11, 12, 15], spatial phase detection (SPD) [18], phase locked loop (PLL) [10] and other analysis methods [9, 19].

Among these methods, phase shifting profilometry (PSP) is one of the most popular approach to carrying out three-dimensional reconstruction, because it is not sensitive to the

background and the reflection factor of surfaces. With PSP, N ($N \geq 3$) frames of fringe patterns with $2\pi/N$ phase shift between each other are sequentially projected onto the reference plane and the surface of the object, and captured by a CCD camera. Then the N images are processed by using PSP algorithm and the height distribution of the surface can be calculated.

As mentioned above, PSP needs at least three steps of phase shifting. Therefore, three-step PSP is very important for PSP technique because it provides the smallest number of phase shifting steps, the least amounts of acquired images and the shortest measurement time when using PSP technique. Additionally, three-step PSP is the only method to implement colour channel based PSP [6].

Meanwhile, in recent years, because of the simplicity and controllability, digital projection is widely used to generate sinusoidal fringe patterns [3, 5, 6, 8]. However, when employing digital projectors, nonlinear distortions are unavoidably introduced and result in visible measurement errors [3, 5], which has been theoretically analyzed in [5, 7]. As nonlinear distortions result in the harmonics components, digital filters are commonly utilized to eliminate the harmonics and pick fundamental components. However, as pointed out by Hu et al., because ideal digital lowpass (or bandpass) filters are physically unrealizable, the signals filtered by lowpass filters are still not be pure sinusoidal [5]. Due to the non-ideal lowpass filtering, compared with the fundamental component, the harmonics higher than third order can be ignored, but the second and the third order harmonics might still exist in the filtered fringe patterns. Meanwhile, as three-step PSP is very sensitive to the second order harmonic but not sensitive to the third order harmonic [4, 5], in order to further improve the reconstruction accuracy for three-step PSP, the influence of the second order harmonics has to be eliminated. Huang et al. have proposed a 'double three-step PSP' method to reduce the influence of the second order harmonics. However, with this approach three

extra images are needed, which is as many as six-step PSP method does, so that extra images and measurement time are required. In this paper, we present a new method to achieve accurate three-dimensional surface reconstruction based on three-step PSP without introducing extra images.

This paper is organized as follows. In section 2, we briefly review the principle of PSP and analyze the errors introduced by the second order harmonics. In section 3 the improved three-step PSP (I3PSP) is proposed. Based on the proposed approach, simulations are performed to demonstrate the improvement of the proposed I3PSP in Section 4. Section 5 concludes this paper.

2 Principle of PSP and Error Analysis

A schematic diagram of a typical FPP system is shown in Fig.1. For simplicity, we consider a cross section of the

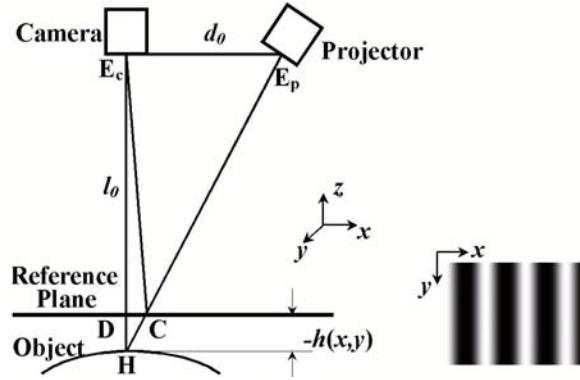


Figure 1. Schematic diagram of FPP system

object surface for a given y coordinate. Hence, the intensity of fringe patterns captured by CCD camera and the height distribution function can be expressed as a function with single variable x . Thus we use $s(x)$ and $d(x)$ to denote the intensity of the projected and deformed fringe pattern respectively and use $h(x)$ to represent the height distribution of the object surface.

In three-step PSP approach, three fringe patterns are sequentially projected onto the reference plane and the surface of the object and captured by a CCD camera. Each one of the three fringe patterns has phase difference of $\frac{2\pi}{3}$ from the others. Meanwhile, because of the existence of nonlinear distortions in the system, high order harmonics are introduced into the captured fringe patterns $s_n(x)$ and $d_n(x)$, which can be expressed as:

$$s_n(x) = \sum_{k=0}^{+\infty} a_k \cos(k \cdot (2\pi f_0 x + \frac{2\pi(n-1)}{3}))$$

$$\text{for } n = 1, 2, 3. \quad (1)$$

$$d_n(x) = \sum_{k=0}^{+\infty} a_k \cos(k \cdot (2\pi f_0 x + \frac{2\pi(n-1)}{3}) + k\phi(x))$$

$$\text{for } n = 1, 2, 3. \quad (2)$$

where f_0 is the spatial frequency of the fringe patterns and $\phi(x)$ is the phase shift caused by the profile of the object, which contains the information about the height distribution of objects. a_k is the amplitude of the k -th order harmonics of the fringe patterns. Obviously, $k = 0$ represents the direct component. n denotes the n -th step of the PSP.

In order to eliminate harmonics and obtain fundamental components of $s_m(x)$ and $d_m(x)$, lowpass filters are commonly utilized. If the lowpass filter is ideal, the dc and fundamental components of $s_n(x)$ and $d_n(x)$ will be picked up [1], which can be expressed as:

$$\bar{s}_n(x) = a_0 + a_1 \cos(2\pi f_0 x + \frac{2\pi(n-1)}{3})$$

$$\text{for } n = 1, 2, 3. \quad (3)$$

$$\bar{d}_n(x) = a_0 + a_1 \cos(2\pi f_0 x + \frac{2\pi(n-1)}{3} + \phi(x))$$

$$\text{for } n = 1, 2, 3. \quad (4)$$

Then phase map $\phi(x)$ and the height distribution of the object can be calculated by following equations:

$$\bar{S} = \tan(2\pi f_0 x) = \frac{\bar{S}_A}{\bar{S}_B}$$

$$= \frac{-\sum_{n=1}^3 \bar{s}_n(x) \sin \frac{2\pi(n-1)}{3}}{\sum_{n=1}^3 \bar{s}_n(x) \cos \frac{2\pi(n-1)}{3}} \quad (5)$$

$$\bar{D} = \tan(2\pi f_0 x + \phi(x)) = \frac{\bar{D}_A}{\bar{D}_B}$$

$$= \frac{-\sum_{n=1}^3 \bar{d}_n(x) \sin \frac{2\pi(n-1)}{3}}{\sum_{n=1}^3 \bar{d}_n(x) \cos \frac{2\pi(n-1)}{3}} \quad (6)$$

$$\phi(x) = \text{unwrap}(\arctan(\bar{D}))$$

$$- \text{unwrap}(\arctan(\bar{S})) \quad (7)$$

$$h(x) = \frac{l_0 \phi(x)}{\phi(x) - 2\pi f_0 d_0} \quad (8)$$

where \bar{S} and \bar{D} are intermediate variables. d_0 and l_0 are the distance from the camera to the projector and the reference plane, respectively. *unwrap* denotes the operation of phase unwrapping.

However, as mentioned in Section 1, because of the non-ideal lowpass filters, \bar{s}_n and \bar{d}_n can not be exactly obtained. The second order harmonic components will exist in the filtered signals and have the strongest power in harmonics.

Meanwhile, as three-step PSP is not sensitive to the third order harmonics and the power of the harmonics higher than the third order will be weak enough to be ignored, for our analysis, the actually obtained signals \hat{s}_n and \hat{d}_n can be expressed as:

$$\begin{aligned}\hat{s}_n(x) &= a_0 + a_1 \cos(\theta(x) + \frac{2\pi(n-1)}{3}) \\ &\quad + b \cos(2\theta(x) + 2 \cdot \frac{2\pi(n-1)}{3}) \\ &\quad \text{for } n = 1, 2, 3.\end{aligned}\quad (9)$$

$$\begin{aligned}\hat{d}_n(x) &= a_0 + a_1 \cos(\theta(x) + \frac{2\pi(n-1)}{3}) + \phi(x) \\ &\quad + b \cos(2\theta(x) + 2 \cdot \frac{2\pi(n-1)}{3}) + 2 \cdot \phi(x) \\ &\quad \text{for } n = 1, 2, 3.\end{aligned}\quad (10)$$

where $\theta(x) = 2\pi f_0 x$ and b is the amplitude of the second order harmonic after the lowpass filtering. If we use \hat{s}_n and \hat{d}_n instead of \bar{s}_n and \bar{d}_n to calculate phase map $\phi(x)$ and height distribution $h(x)$, errors will be introduced [5, 7].

3 Improved Three-step PSP

As analyzed in Section 2, we have to design an algorithm to reconstruct phase map from $\hat{s}_n(x)$ and $\hat{d}_n(x)$ and at the same time eliminate the errors introduced by the second order harmonics.

If we use \hat{s}_n instead of \bar{s}_n to calculate the numerator of Eq.(5), we will have:

$$\begin{aligned}\hat{S}_A &= -\sum_{n=1}^3 \hat{s}_n(x) \sin \frac{2\pi(n-1)}{3} \\ &= -[a_0 + a_1 \cos(\theta + \frac{2\pi}{3}) + b \cos(2\theta + \frac{4\pi}{3})] \cdot \sin \frac{2\pi}{3} \\ &\quad - [a_0 + a_1 \cos(\theta + \frac{4\pi}{3}) + b \cos(2\theta + \frac{8\pi}{3})] \cdot \sin \frac{4\pi}{3} \\ &= \frac{3}{2} \cdot [a_1 \sin(\theta) - b \sin(2\theta)]\end{aligned}\quad (11)$$

and for calculating the denominator of Eq.(5), we can have:

$$\begin{aligned}\hat{S}_B &= \sum_{n=1}^3 \hat{s}_n(x) \cos \frac{2\pi(n-1)}{3} \\ &= a_0 + \cos \theta \\ &\quad + [a_0 + a_1 \cos(\theta + \frac{2\pi}{3}) + b \cos(2\theta + \frac{4\pi}{3})] \cdot \cos \frac{2\pi}{3} \\ &\quad + [a_0 + a_1 \cos(\theta + \frac{4\pi}{3}) + b \cos(2\theta + \frac{8\pi}{3})] \cdot \cos \frac{4\pi}{3} \\ &= \frac{3}{2} \cdot [a_1 \cos(\theta) + b \cos(2\theta)]\end{aligned}\quad (12)$$

It can be seen that both of \hat{S}_A and \hat{S}_B are influenced by the second order harmonics. Fortunately, making a good

use of the relationship between \hat{S}_A and \hat{S}_B , the terms of the second order harmonic can be removed. Let us try to calculate \hat{P} :

$$\begin{aligned}\hat{P} &= (\hat{S}_A)^2 + (\hat{S}_B)^2 \\ &= \frac{9}{4} [a_1 \sin(\theta) - b \sin(2\theta)]^2 \\ &\quad + \frac{9}{4} [a_1 \cos(\theta) + b \cos(2\theta)]^2 \\ &= \frac{9}{4} [a_1^2 + b^2 + 2a_1b(\cos \theta \cos 2\theta - \sin \theta \sin 2\theta)] \\ &= \frac{9}{4} [a_1^2 + b^2 + 2a_1b \cos(3\theta)]\end{aligned}\quad (13)$$

By simply removing the direct component of \hat{P} , we can have a signal P whose frequency is the three times of fundamental frequency of the fringe pattern:

$$P = \frac{9}{2} a_1 b \cos(3\theta)\quad (14)$$

Obviously, by obtaining P the second order harmonic has been completely removed and only the signal with three times of fundamental frequency is remained.

Similarly, using $\hat{d}_n(x)$ instead of $\bar{d}_n(x)$ we can calculate \hat{D}_A and \hat{D}_B respectively:

$$\hat{D}_A = \frac{3}{2} \cdot [a_1 \sin(\theta + \phi) - b \sin(2\theta + 2\phi)]\quad (15)$$

$$\hat{D}_B = \frac{3}{2} \cdot [a_1 \cos(\theta + \phi) + b \cos(2\theta + 2\phi)]\quad (16)$$

and

$$\begin{aligned}\hat{Q} &= (\hat{D}_A)^2 + (\hat{D}_B)^2 \\ &= \frac{9}{4} [a_1^2 + b^2 + 2a_1b \cos(3\theta + 3\phi(x))]\end{aligned}\quad (17)$$

By removing the direct component of \hat{Q} , we can have:

$$Q = \frac{9}{2} a_1 b \cos(3\theta + 3\phi(x))\quad (18)$$

Hence, the phase map $\phi(x)$ can be easily obtained from P and Q . Let us denote the analytic signals of P and Q by \tilde{P} and \tilde{Q} , respectively and use \tilde{P}^* to represent the conjugate of \tilde{P} . The phase map $\phi(x)$ can be calculated by:

$$\phi(x) = \frac{\mathbf{Im}[\ln(\tilde{Q} \cdot \tilde{P}^*)]}{3}\quad (19)$$

where \mathbf{ln} denotes the natural logarithm, and \mathbf{Im} represents the imaginary part of a complex number. It can be seen that the phase map can be exactly retrieved and no extra errors are introduced.

In summary, the proposed I3PSP is implemented by following steps:

1. Apply lowpass filtering to the captured signals s_n and d_n to obtain \hat{s}_n and \hat{d}_n ,
2. Based on \hat{s}_n and \hat{d}_n to calculate $\hat{S}_A, \hat{S}_B, \hat{D}_A$ and \hat{D}_B by using Eqs.(11),(12),(15) and (16), respectively,
3. Calculate P and Q from $\hat{S}_A, \hat{S}_B, \hat{D}_A$ and \hat{D}_B ,
4. Retrieve phase map by using Eq(19),
5. Reconstruct the hight distribution of the surface by Eq.(8).

4 Simulations

In this section, simulations are performed to demonstrate the significantly improved reconstruction accuracy of using I3PSP algorithm compared with traditional three-step PSP. In our simulation, we use a paraboloid object surface whose maximum height is 160mm, which is shown in Fig.2(d).

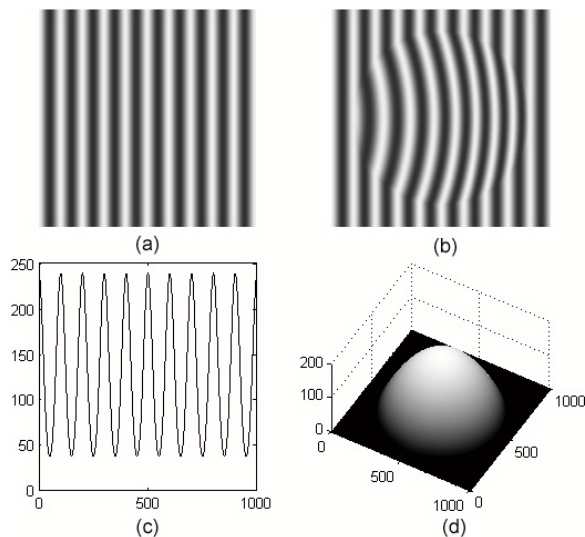


Figure 2. Simulated fringe patterns and surface

Meanwhile, we assume that the amplitude of fundamental component is 100, and after lowpass filtering, the second order harmonic has only -20db of power compared with the fundamental component, which is expressed as:

$$\hat{s}_n(x) = 128 + 100 \cdot \cos\left(2\pi f_0 x + \frac{2\pi(n-1)}{3}\right) + 10 \cdot \cos\left(2\pi \cdot (2f_0)x + 2 \cdot \frac{2\pi(n-1)}{3}\right) \quad \text{for } n = 1, 2, 3. \quad (20)$$

where f_0 is the spatial frequency of the fringe pattern, which is assumed to be 10/meter in our simulation. i.e. the spatial period of the fringe pattern is assumed to be 100mm. Meanwhile, we assume l_0 and d_0 in Fig.1 equal to 5 meters and 2 meters respectively. The spatial resolution of the captured image is assumed to be 1 pixel/mm.

Corresponding to Eq.(20), the fringe pattern deformed by the profile of the object can be expressed as: [13, 14]

$$\hat{d}_n(x) = 128 + 100 \cos\left(2\pi f_0 x + \frac{2\pi(n-1)}{3} + \phi(x)\right) + 10 \cos\left(2\pi \cdot (2f_0)x + 2 \cdot \frac{2\pi(n-1)}{3} + 2\phi(x)\right) \quad \text{for } n = 1, 2, 3. \quad (21)$$

where $\phi(x)$ is the phase shift caused by the object surface. The fringe patterns $\hat{s}_n(x)$ and $\hat{d}_n(x)$ are shown in Fig.2(a) and (b) respectively. Fig.2(c) plots a cross section of the fringe pattern demonstrated in Fig.2(a). In fact, we can hardly distinguish this fringe pattern from a pure sinusoidal one, although it has been distorted by the second order harmonic. However, this slight distortion will result in notable reconstruction errors when using traditional three-step PSP. The reconstruction result by using three-step PSP is shown in Fig.3. It can be seen that the reconstructed surface by

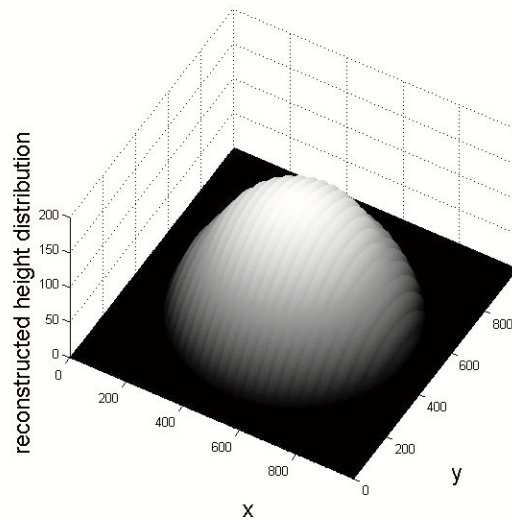


Figure 3. Reconstruction result by using traditional three-step PSP

using PSP method is jagged and not smooth.

In contrast, by our proposed I3PSP method, we can obtain a much smoother reconstruction result as shown in

Fig.4. In order to show the improvement of the proposed

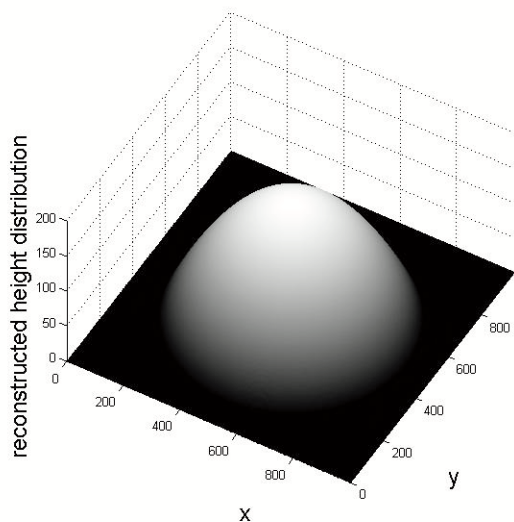


Figure 4. Reconstruction result by using I3PSP

I3PSP more clearly, we select a cross section of the surface to compare the reconstruction results as shown in Fig.5. Solid lines in Fig.5(a) and (b) are the surface reconstructed by using the traditional three-step PSP and using the proposed I3PSP, respectively. The dashed lines denote the true values of the object surface. We can see that reconstruction result by using traditional three-step PSP has undesired ripples, which implies visible errors are introduced although the second order harmonic has only -20db of power compared with the fundamental component, whereas as shown in Fig.5(b), the reconstruction result by using the proposed I3PSP is almost identical to the true value of the height distribution.

5 Conclusions

In this paper, we proposed a new algorithm, called I3PSP, to reconstruct three-dimensional surface based on three-step phase shifting profilometry technique. Compared with traditional three-step PSP method, the proposed I3PSP can significantly reduce the influence of the second order harmonics, which is the main error source of the traditional three-step PSP. The measurement accuracy using three-step PSP technique can be much improved by the proposed I3PSP. The effectiveness and the improvement of I3PSP has been completely confirmed by our simulation results.

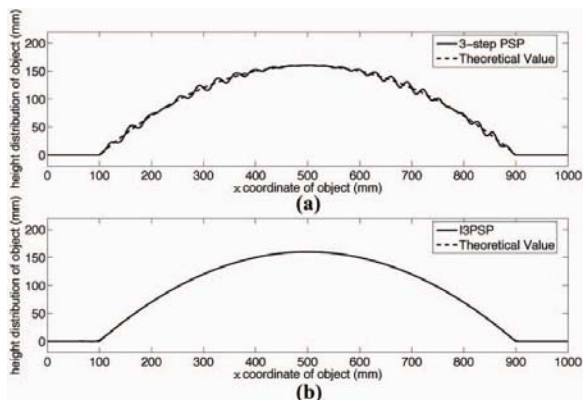


Figure 5. A cross section of the surface reconstructed by three-step PSP and I3PSP

References

- [1] F. Berryman, P. Pynsent, and J. Cubillo. A theoretical comparison of three fringe analysis method for determining the three dimensional shape of an object in the present of noise. *Optics and Lasers in Engineering*, 39:35–50, 2003.
- [2] R. Green, J. Walker, and D. Robinson. Investigation of the fourier-transform method of fringe pattern analysis. *Optics and Lasers in Engineering*, 8:29–44, 1988.
- [3] H. Guo, H. He, and M. Chen. Gamma correction for digital fringe projection profilometry. *Applied Optics*, 43:2906–2914, May 2004.
- [4] K. Hibino, B. F. Oreb, D. I. Farrant, and K. G. Larkin. Phase shifting for nonsinusoidal waveforms with phase-shift errors. *Journal of the Optical Society of America A*, 12:761–768, April 1995.
- [5] Y. Hu, J. Xi, E. Li, J. Chicharo, and Z. Yang. Three-dimensional profilometry based on shift estimation of projected fringe patterns. *Applied Optics*, 45:678–687, February 2006.
- [6] P. Huang, Q. Ho, F. Jin, and F. Chiang. Colour-enhanced digital fringe projection technique for high-speed 3-D surface contouring. *Opt Eng*, 38:1065–1071, 1999.
- [7] P. S. Huang, Q. J. Hu, and F.-P. Chiang. Double three-step phase-shifting algorithm. *Applied Optics*, 41:4503–4509, August 2002.
- [8] L. Kinell. Multichannel method for absolute shape measurement using projected fringes. *Optics and Lasers in Engineering*, 41:57–71, 2004.
- [9] A. Moore and F. Mendoza-Santoyo. Phase demodulation in the space domain without a fringe carrier. *Optics and Lasers in Engineering*, 23:319–330, 1995.
- [10] R. Rodriguez-Vera and M. Servin. Phase locked loop profilometry. *Optics and Lasers Technology*, 26:393–398, 1994.
- [11] V. Srinivasan, H. Liu, and M. Halioua. Automated phase-measuring profilometry of 3-D diffuse objects. *Applied Optics*, 23:3105–3108, 1984.

- [12] H. Su, J. Li, and X. Su. Phase algorithm without the influence of carrier frequency. *Optics Engineering*, 36:1799–1805, 1997.
- [13] X. Su and W. Chen. Fourier transform profilometry: a review. *Optics and Lasers in Engineering*, 35:263–284, 2001.
- [14] X. Su, W. Chen, Q. Zhang, and Y. Chao. Dynamic 3-D shape measurement method based on ftp. *Optics and Lasers in Engineering*, 36:49–64, 2001.
- [15] X. Su, W. Zhou, von Bally G, and D. Vukicevic. Automated phase-measuring profilometry using defocused projection of ronchi grating. *Optics Communication*, 94:561–573, 1992.
- [16] M. Takeda, H. Ina, and S. Kobayashi. Fourier-transform method of fringe-pattern analysis for computer-based topography and interferometry. *Journal of the Optical Society of America A*, 72:156–160, 1982.
- [17] M. Takeda and K. Mutoh. Fourier transform profilometry for the automatic measurement of 3-D object shapes. *Applied Optics*, 22:3977–3982, 1983.
- [18] S. Toyooka and Y. Iwaasa. Automatic profilometry of 3-D diffuse objects by spatial phase detection. *Applied Optics*, 25:1630–1633, 1986.
- [19] J. Villa, M. Servin, and L. Castillo. Profilometry for the measurement of 3-D object shapes based on regularized filters. *Optics Communication*, 161:13–18, 1999.
- [20] J. Yi and S. Huang. Modified fourier transform profilometry for the measurement of 3-D steep shapes. *Optics and Lasers in Engineering*, 27:493–505, 1997.